

# A biogenerated polymetallic catalyst from society's wastes

## ABSTRACT

**Aims:** Preparation of the new metals-polymeric composite, Met<sub>x</sub>-EPS (I), to be used as a green catalyst in water or in two-phase aqueous conditions.

**Study design:** Recovery and valorization of polymetallic wastes to obtain directly new catalysts using a microorganism to explore their application in removal of difficult and dangerous chemical pollutants present in aqueous environment.

**Place and Duration of Study:** Dipartimento di Scienze Molecolari e Nanosistemi, Università Ca' Foscari Venezia, Venezia Mestre, Italy; University of Nova Gorica, Nova Gorica, Slovenia, Institut Jozef Stefan, Ljubljana, Slovenia and Department of Biology, Biotechnical Faculty, University of Ljubljana, Ljubljana, Slovenia, between February 2018 and January 2019.

**Methodology:** For the preparation of Met<sub>x</sub>-EPS (I), the metals source was an exhausted catalytic converter that was grinded and treated with an acidic solution at room temperature. After filtration, the solution was concentrated, neutralized and added to a broth of *Klebsiella oxytoca* DSM 29614 to produce (I) where metals are embedded in a peculiar polysaccharide structure. The composite was easily recovered from the fermentation broth and purified. The process protocol was verified many times and was shown to be reproducible satisfactorily. The % recovery of metals, originally present in the converter, was good as determined by atomic absorption. The morphology and the chemical state of main metals in (I) were investigated by X-ray absorption spectroscopy methods (XANES and EXAFS). No metallic alloy seems to be evident.

**Results:** As first application of (I) as catalyst, the hydrodechlorination treatment of polychlorinated biphenyls (PCBs) was studied in water/methanol. A significant removal of higher chlorinated congeners was observed working at 1MPa of hydrogen and 60°C. This result improves significantly and surprisingly the methodology, previously studied by us using mono- or bi-metals embedded in the same polysaccharide moiety, indicating that positive synergies among the different metals were operating.

**Conclusion:** The preparation of this new polymetallic species embedded in a polysaccharide moiety starting from spent catalytic converters represents an alternative valorisation of metallic wastes. Moreover, a synergic effect was exerted by the different metals when the catalyst Met<sub>x</sub>-EPS (I) was used in the hydrodechlorination treatment of polychlorinated biphenyls (PCBs) in water/methanol. Finally, a promising preliminary proof of concept for the removal of polychlorinated aromatic pollutants even in contaminated aqueous sites was carried out.

**Keywords:** Metals-polymeric composite; biogenerated polymetallic exopolysaccharide; new catalyst from metallic wastes; hydrodechlorination of PCBs in water

## 1. INTRODUCTION

As now requested by the circular economy, valuable metals have to be recovered from industrial scraps, such as for example exhausted catalytic converters. Current approaches to

19 treat relevant metallic waste categories are based on pyrometallurgical, hydrometallurgical  
20 or bio-hydrometallurgical methods, which present advantages and disadvantages in terms  
21 of energy consumption, use of special equipments and difficulty in the purification [1,2].  
22 Then a following treatment is necessary to produce metallic catalysts. To overcome these  
23 drawbacks and to obtain directly a composite useful as catalyst, our protocol at first treats  
24 grinded exhausted catalytic converters at room temperature with a concentrated acidic  
25 solution, such as aqua regia or 80% nitric acid, to dissolve metals as ions and, after filtration  
26 of the solid residue, concentration and neutralization of the solution, takes advantage of the  
27 property of a plurimetal resistant microorganism *Klebsiella oxytoca* DSM 29614. This  
28 microorganism is able to generate, in the presence of heavy metal cations, a specific  
29 capsular exopolysaccharide (EPS) which may embed them and then be extruded from the  
30 cell so to be easily purifiable [3-4]. So a new metals-polymeric composite, Met<sub>x</sub>-EPS (I) was  
31 obtained from exhausted catalytic converters and, after characterization with different  
32 methods, its catalytic activity and a possible synergic effect due to the presence of different  
33 metals embedded in EPS was verified in the hydrodechlorination treatment of a methanolic  
34 solution of polychlorinated biphenyls (PCBs) in distilled water and in a sample of polluted  
35 sea water (Mar Piccolo, Taranto, Italy). The results were compared with those recently  
36 obtained by us using Pd-EPS or Pd,Fe-EPS [5].

## 37 38 **2. MATERIAL AND METHODS / EXPERIMENTAL DETAILS / METHODOLOGY**

### 39 40 **2.1 Materials and Instrumentation**

41 Nutrient broth (Difco), n-hexane (pesticide grade; Romil), PCB standards (AccuStandard)  
42 were utilised. Aroclor 1260 and the other reagents were Sigma-Aldrich products and used as  
43 received. The total amounts of elements were determined versus their relative standards  
44 solutions by inductively coupled plasma atomic emission spectrometry (ICP-AES) (Optima  
45 3100, Perkin Elmer). The FT-IR spectra (KBr pellets) of Met<sub>x</sub>-EPS were recorded on an FT-  
46 IR Nicolet Magna 750 instrument. X-ray absorption spectra were measured on of Met<sub>x</sub>-EPS  
47 sample in the energy range of K or L3 absorption edges of constituent metal cations (Pd K-  
48 edge (24350 eV), Rh K-edge (23220 eV), Zr K-edge (17998 eV), Pt L3 edge (11564 eV), Ce  
49 L3 edge (5724 eV)) to obtain corresponding XANES (X-ray Absorption Near Edge Structure)  
50 and EXAFS (Extended X-ray Absorption Fine Structure) spectra of the investigated  
51 elements. The Met<sub>x</sub>-EPS sample was prepared in the form of homogeneous self-standing  
52 pellets, each optimised to provide the total absorption thickness ( $\mu$ d) of about 1.5 above the  
53 investigated absorption edges. All absorption spectra were measured at room temperature in  
54 transmission detection mode at two different synchrotron radiation facilities (Zr, Pt and Ce at  
55 XAFS beamline at Elettra in Trieste, Italy; Pd and Rh at BL22 (Claess) beamline of ALBA in  
56 Barcelona, Spain); a Si (111) double crystal monochromator was used at the XAFS  
57 beamline of the Elettra and a Si(311) at BL22 of ALBA. The intensity of the monochromatic  
58 X-ray beam was measured by three consecutive ionization detectors. The samples were  
59 placed between the first pair of detectors. The exact energy calibration was established with  
60 simultaneous absorption measurement on the corresponding reference metal foil placed  
61 between the last pair of detectors. Absolute energy reproducibility of the measured spectra  
62 was  $\pm 0.03$  eV. The absorption spectra were measured within the interval [-150 eV to 1000  
63 eV] relative to the investigated absorption edge. In the XANES region, equidistant energy  
64 steps of 0.5 eV were used, while for the EXAFS region, equidistant k-steps ( $\Delta k = 0.03 \text{ \AA}^{-1}$ )  
65 were adopted, with an integration time of 1 s per step. The quantitative analysis of XANES  
66 and EXAFS spectra is performed with the IFEFFIT program package [6] in combination with  
67 FEFF6 program code [7] for ab initio calculation of photoelectron scattering paths. The  
68 determination of PCB congeners was performed in full scan mode on a fused silica capillary  
69 column (HP5-MS 30 m, 0.25 mm x 0.25 mm; Agilent Technologies) installed in a  
70 ThermoFinnigan (Trace GC 2000) coupled to a quadrupole mass spectrometer  
71 (ThermoFinnigan Trace MS), using the same conditions described in our previous work [5].

72

73

74

## 2.2 Recovery of acidic metallic solutions from grinded exhausted catalytic converters and preparation of a new metals-polymeric composite (I)

75

76

77

78

79

80

81

82

83

84

85

86

87

88

89

90

91

92

93

94

95

## 2.3 Element determination in a new metals-polymeric composite (I)

96

97

98

99

Samples (1 mg) of dry pulverized polymetallic composites were digested with 2 ml of aqua regia, heating the mixture at 60°C until a complete dissolution for element determination. The recovery yield of the main metals is reported in **Table A**.

100

101

## 2.4 Optimized protocol of hydrodechlorination of Aroclor 1260 using the new catalyst (I)

102

103

104

105

106

107

108

109

110

111

112

113

114

115

A suitable amount of Met<sub>x</sub>-EPS (I) to obtain a substrate/Pd ≈ 8/1 mol ratio (8.8 mg) was stirred in a Schlenk tube under nitrogen in 4 ml of distilled water or 4 ml of Mar Piccolo (Taranto, Italy) water for about 10 min. A solution of 7 mg of Aroclor 1260 (~0.0195 mmol assuming MW 358 as medium value) in 2 ml of methanol was then added to the aqueous phase as well as 1.7 mg (0.021 mmol) of ammonium acetate. The Schlenk tube was then transferred into a 150 ml stainless steel autoclave under nitrogen, pressurized with 1 MPa of H<sub>2</sub>, instead of 3MPa used previously with Pd-EPS or Pd,Fe-EPS [5], and stirred at 60°C for 20 h. The reactor was then cooled to room temperature and opened under nitrogen. Then, the organic products were separated from the catalyst extracting them from the aqueous phase with 10 mL of n-hexane. The procedure of extraction was repeated three times. The organic phases were collected and dried on Na<sub>2</sub>SO<sub>4</sub>, then concentrated using a nitrogen flow (Turbovap 2, Caliper Science) and analyzed by GC-MS.

116

## 3. RESULTS AND DISCUSSION

117

118

119

120

### 3.1 Catalyst characterization

121

The results of elemental determination are reported in **Table A**.

122

123  
124

**Table A.** Main metals extracted from exhausted catalytic converters and present in Met<sub>x</sub>-EPS<sup>a</sup>.

Analyzed Metals	C (mg/L) HNO <sub>3</sub> (n.a.) sol. (inc. ±10%)	C (mg/L) aqua regia (a.r.) sol. (inc. ±10%)	(Met <sub>x</sub> EPS) <sub>n.a.</sub> Metal recovery yield% <sup>b</sup>	(Met <sub>x</sub> EPS) <sub>a.r.</sub> Metal recovery yield% <sup>b</sup>
Pd	428	748	89	99
Pt	31.9	479	81	83
Rh	2.07	111	84	85
Al	1623	2413	80	>99
Ce	nd	2158	nd	99
Zr	nd	nd	nd	nd
W	121	174	29	10

125 <sup>a</sup> Experimental conditions: 20 g of exhausted catalytic converter; 400 ml of 80% HNO<sub>3</sub> or  
126 aqua regia; T = 20°C; t = 24 h; final volume of the acidic solution after distillation = 80 ml. <sup>b</sup>  
127 (Amount of metal encapsulated in EPS)/(amount of metal present in the starting acidic  
128 solution)%. nd = not determined

129

130 Even if the aqua regia treatment is, as expected, more efficient to extract metals from  
131 exhausted catalytic converters, the % of recovery of metals, bonded or encapsulated in the  
132 new composite, after the biological treatment, is not significantly affected and is very high  
133 (80->99%) with the exception of tungsten (**Table A**).

134

135 As already described in more detail [S. Paganelli et al., Ca' Foscari University, Venice, Italy,  
136 paper submitted to ChemistrySelect], Met<sub>x</sub>-EPS (**I**) was characterized by FT-IR and by the x-  
137 ray absorption spectroscopy methods XANES and EXAFS. The IR spectrum (**Appendix**,  
138 **Fig. 1**) confirmed the presence of metals bound to capsular EPS. It looks quite similar to the  
139 spectrum of a previous prepared Pd-EPS [4] but with a very intense sharp band at 1384  
140 cm<sup>-1</sup>. The intense symmetric stretching of COO<sup>-</sup> vibration to 1384 cm<sup>-1</sup>, on the basis of  
141 literature, should demonstrate, in our opinion, that carboxyl group was a contributor in the  
142 sorption of metals [8, 9]. In the region between 1550-1650 cm<sup>-1</sup> it is possible to observe two  
143 peaks, one of them or both could be due to the asymmetric stretching of COO<sup>-</sup> vibration  
144 bounded to metals [8]. Indeed the EPS is formed by an eptameric structure with two D-  
145 glucuronic acids, four L-rhamnose, and one D-galactose [10]. However it is not possible to  
146 exclude also contribution of nitrogen species such as any nitrogen heterocyclic compounds  
147 eventually formed during the fermentation or membrane protein amide bonds [9]. Finally,  
148 the other intense peak at 1065 cm<sup>-1</sup>, as it was already observed for other similar metal EPS,  
149 is to attribute to phosphate groups [4, 9].

149

150 The presence of metals bounded to capsular EPS and valence and structural information of  
151 metal cations in the Met<sub>x</sub>-EPS complex at the atomic scale were confirmed by x-ray  
152 absorption spectroscopy methods XANES and EXAFS [S. Paganelli et al., Ca' Foscari  
153 University, Venice, Italy, paper submitted to ChemistrySelect]. It is known that, in the XANES  
154 spectrum, an increase of oxidation state results in a shift of each absorption feature to higher  
155 energies [4,11]. The Pd K-edge profile of the Pd in the Met<sub>x</sub>-EPS complex are identical  
156 to the Pd XANES spectrum of the Pd metal foil with fcc crystalline structure and also to FePd-  
157 EPS(A), FePd-EPS(B) and Pd-EPS samples, previously reported by us [4]. It clearly  
158 indicates that palladium also in (**I**) is predominantly as Pd (0) (**Appendix, Fig. 2a**).

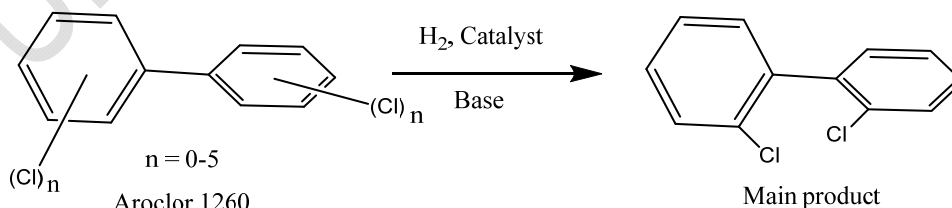
158 Results of Pd K-edge EXAFS analysis (**Appendix, Fig. 2b**) suggested that Pd in (I) is in the  
159 form of Pd(0) metallic nano-particles with fcc crystalline structure, similar to that found in  
160 mono- and bi-metallic (Pd-EPS and FePd-EPS) samples from previous investigations [4].  
161 However smaller nano-clusters of Pd metal are formed and the average size of Pd metal  
162 nanoparticles is less than 1 nm (**Appendix, Table 1**). Furthermore, in EXAFS analysis of Pd  
163 neighborhood, we found that part of Pd atoms is coordinated to oxygen atoms at about 1.97  
164 Å which is characteristic for Pd oxides (**Appendix, Table 1**). So it is possible that about 10%  
165 of Pd atoms is in the form of PdOx nanoparticles simply encapsulated in the polysaccharide  
166 moiety or that Pd atoms located on the surface of the Pd metallic nanoparticles may be  
167 bonded to the OH or COOH groups of EPS. The results (**Appendix, Fig. 2b**) are similar, but  
168 not identical, to those observed on mono- and bi-metallic samples [4].  
169 The Pt L3-edge XANES analysis would suggest that there are two forms of Pt in (I), one is  
170 metallic Pt(0) nanoparticles (about 36 %), as expected, the other in the form of a Pt(II)  
171 complex bound to two Cl atoms and two nitrogen atoms like in PtCl<sub>2</sub>(pyridine)<sub>2</sub> (**Appendix,**  
172 **Fig 3a**) [12]. Pt L3-edge EXAFS results strongly support this finding (**Appendix, Fig 3b,**  
173 **Table 2**). The results clearly suggest that microorganism *Klebsiella oxytoca* encapsulates Pt  
174 species in EPS partly in the form of metallic Pt(0) nanoparticles and partly in the form of  
175 complexes structurally similar to PtCl<sub>2</sub>(pyridine)<sub>2</sub>. It is difficult to have a clear-cut explanation  
176 for the latter form. Maybe PtCl<sub>2</sub>, originally added to the fermentation broth, can bind to  
177 nitrogen heterocyclic species, e.g. piperazine derivatives, probably formed during the  
178 fermentation process [13].  
179 The Ce L3-edge XANES analysis (**Appendix, Fig. 4**) and the comparison with CeVO<sub>4</sub> and  
180 CeO<sub>2</sub> XANES spectra showed that all Ce in the Met<sub>x</sub>-EPS sample is in the form of three  
181 valent Ce cations, most probably in the form of Ce<sup>3+</sup> oxide nanoparticles [14]. Finally the  
182 results of Zr and Rh EXAFS analysis of Met<sub>x</sub>-EPS sample (**Appendix, Figs. 5 and 6**)  
183 suggested that both elements, Zr and Rh, are in oxidized form, as a mixture of different Zr  
184 and Rh nano-oxides. Zr-Zr distances are characteristic for Zr oxides [15] while Rh-Rh  
185 distances are characteristic for crystalline Rh<sub>2</sub>O<sub>3</sub> [16]. Also Ce, Zr or Rh cations  
186 coordination to OH and COOH groups cannot be excluded.

187  
188  
189

### 190 3.2 Catalyst activity

191 Removal of polychlorinated pollutants present in water by catalysed hydrodechlorination is  
192 still a challenging target due to the presence of different catalyst poisons. As part of our  
193 research activity in environmental remediation and in finding potential sustainable protocols  
194 using heterogeneous water compatible catalysts we had recently studied the  
195 hydrodechlorination of a methanolic solution of Aroclor 1260 (a reference PCB mixture) with  
196 Pd-EPS and Fe,Pd-EPS in pure distilled water in the presence of ammonium acetate [5]  
197 (**Scheme 1**).

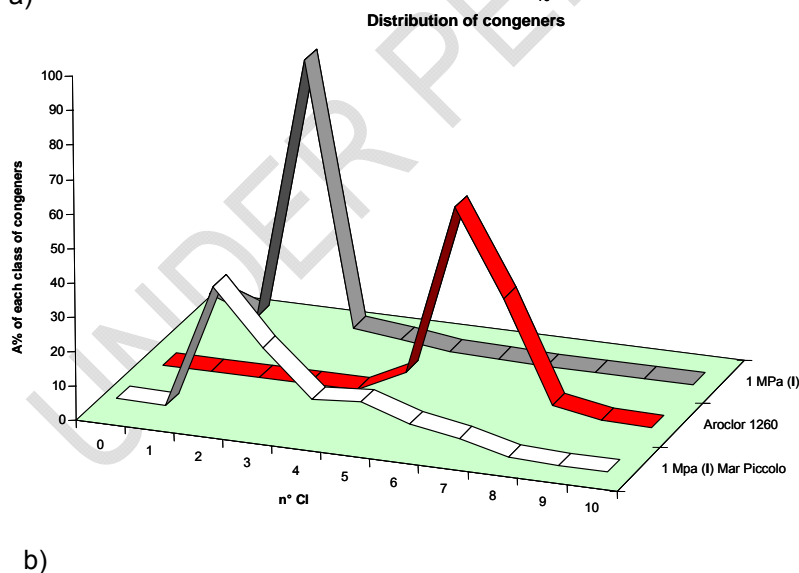
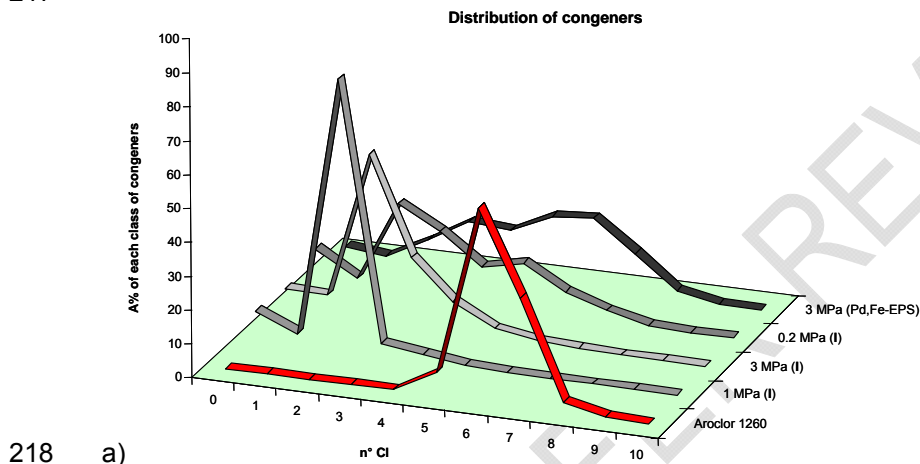
198  
199



200  
201  
202  
203

**Scheme 1.** Hydrodechlorination of Aroclor 1260.

204 An improvement in the dehalogenation reaction using the bimetallic catalyst had been  
 205 observed working at a pressure of 3MPa of hydrogen with a substrate/catalyst 8/1  
 206 ratio (referred to Pd amount), at 60°C in 20 h, but a relevant amount of Cl<sub>5</sub>-Cl<sub>7</sub> congeners  
 207 was still present. Therefore we were encouraged to test this new polymetallic (Met<sub>x</sub>-EPS) (I)  
 208 on the same substrate to try to improve our previous results, working either in pure distilled  
 209 water or diluting this PCBs mixture in a sample of polluted sea water taken from Mar Piccolo  
 210 (Taranto, Italy) which contained also other pollutants such as PAHs and heavy metals. Quite  
 211 surprising, very stimulating and promising results were achieved working under much milder  
 212 reaction conditions. As shown in Fig. 1a it was possible to obtain a complete removal of  
 213 congeners having a content of chlorine atoms >3 working at a pressure of 1MPa of  
 214 hydrogen with the same substrate/catalyst 8/1 molar ratio (referred to Pd amount). Quite  
 215 satisfactory results were also obtained using a real polluted water spiked with Aroclor 1260  
 216 as depicted in Fig. 1b.  
 217



219  
 220  
 221  
 222  
 223  
 224  
 225  
 226  
 227

**Fig. 1.** Hydrodechlorination of Aroclor 1260 results compared with previous best results [5]:  
 a) in pure water; b) diluting Aroclor 1260 in polluted sea water of Mar Piccolo

228 It indicates that this new catalyst is quite robust and is able of working in water and of  
229 resisting to the poisoning. Synergic positive effects due to the presence of polymetals were  
230 clearly demonstrated either in the hydrodechlorination reaction or in the ability to break  
231 down/reduce the amounts of palladium poisons present in the polluted sea water.  
232 Furthermore PCBs concentrations of some very toxic dioxin-like PCBs congeners: BZ 118,  
233 156, 157, 167, 170, 180, 189 in Aroclor 1260 were reduced to nearly zero (A%) (Table B)  
234 using this new catalyst and it is a significant improvement in the used protocol.  
235  
236  
237  
238  
239

240 **Table B.** PCBs concentrations of some dioxin-like PCBs congeners: BZ 118, 156, 157, 167,  
241 170, 180, 189 in Aroclor 1260 and in the product obtained after hydrogenation in the  
242 presence of Pd, Fe-EPS or Met<sub>x</sub>-EPS(I)  
243

BZ Number of some dangerous PCBs congeners <sup>a</sup>	Aroclor 1260 A %	Pd,Fe-EPS A % (3 MPa of H <sub>2</sub> ) <sup>b</sup>	Met <sub>x</sub> -EPS(I) A % (1 MPa of H <sub>2</sub> )
<b>118</b> (+149)	10.18	5.16	0.04
<b>156</b> (+173)	1.84	0.39	nd
<b>157</b> (+197)	0.31	0.07	nd
<b>167</b>	0.72	0.29	nd
<b>170</b> (+190)	4.25	1.33	nd
<b>180</b>	8.88	3.27	nd
<b>189</b>	0.13	0.02	nd

244 <sup>a</sup> congeners number according to Ballschmiter K, Zell M(1980) Analysis of Polychlorinated  
245 Biphenyls (PCB) by Glass Capillary Gas Chromatography. Fresenius Z Anal Chem 302: 20-  
246 31; <sup>b</sup> see ref. [5]; nd = not detected  
247  
248  
249  
250  
251

## 252 4. CONCLUSION

253  
254 The idea to prepare new polymetallic species embedded in a polysaccharide moiety starting  
255 from spent catalytic converters was realized as a contribution of alternative valorisation of  
256 metallic wastes and direct preparation of new metallic catalysts. Even if no metallic alloy  
257 seems to be evident, nevertheless positive synergies among the different metals were found  
258 when(I) was used as a catalyst in the removal of PCBs by hydrodechlorination reaction,  
259 permitting to work under milder conditions with a better efficacy than previous studies [5].  
260 Finally, a promising preliminary application for the removal of these pollutants even in  
261 contaminated aqueous sites has been carried out, showing that the catalyst is quite robust  
262 and potentially useful for a continuous process.  
263  
264  
265

## 266 COMPETING INTERESTS

267  
268 The authors declare no conflict of interest.

269

270

## REFERENCES

271

272

[1] Jadhav UU, Hocheng H, Achiev J. A review of recovery of metals from industrial waste. *Mat. Manufacturer Eng.* 2012; 54: 159-167.

273

274

[2] Izatt RM, Izatt SR, Bruening RL, Izatt NE, Moyer BA. Challenges to achievement of metal sustainability in our high-tech society. *Chem. Soc. Rev.* 2014; 43: 2451-2475.

275

276

[3] Baldi F, Marchetto D, Paganelli S, Piccolo O. Bio-generated metal binding polysaccharides as catalysts for synthetic applications and organic pollutant transformations.

277

278

*New Biotechnology* 2011; 29: 74-78.

279

280

[4] Arčon I, Paganelli S, Piccolo O, Gallo M, Vogel-Mikuš K, Baldi F. XAS analysis of iron and palladium bonded to a polysaccharide produced anaerobically by a strain of *Klebsiella oxytoca*. *J. Synchrotron Rad.* 2015; 22: 1215-1226.

281

282

[5] Baldi F, Gallo M, Paganelli S, Tassini R, Sperti L, Piccolo O, et al. Hydrodechlorination of Aroclor 1260 in Aqueous Two-phase Mixture Catalyzed by Biogenerated Bimetallic Catalysts. *Int. Res. J. Pure & Appl. Chem.* 2016; 11: 1-9 and loc. ref.

283

284

285

[6] Ravel B, Newville M. ATHENA, ARTEMIS, HEPHAESTUS: data analysis for X-ray absorption spectroscopy using IFEFFIT. *J. Synchrotron Rad.* 2005;12: 537-541.

286

287

[7] Rehr JJ, Albers RC, Zabinsky SI. High-order multiple-scattering calculations of x-ray-absorption fine structure. *Phys. Rev. Lett.* 1992; 69: 3397-3400.

288

289

[8] Papageorgiou SK, Kouvelos EP, Favvas EP, Sapalidis AA, Romanos GE, Katsaros FK. Metal-carboxylate interactions in metal-alginate complexes studied with FTIR spectroscopy. *Carbohydr. Res.* 2010; 345: 469-473.

290

291

292

[9] Tan L, Dong H, Liu X, He J, Xu H, Xie J. Mechanism of palladium(II) biosorption by *Providencia vermicola*. *RSC Adv.* 2017; 7: 7060-7072.

293

294

[10] Leone S, De Castro C, Parrilli M, Baldi F, Lanzetta R. Structure of the Iron-Binding Exopolysaccharide Produced Anaerobically by the Gram-Negative Bacterium *Klebsiella oxytoca* BAS-10. *Eur. J. Org. Chem* 2007; 5183-5189.

295

296

297

[11] Wong J, Lytle FW, Messmer RP, Maylotte DH. K-edge absorption spectra of selected vanadium compounds. *Phys. Rev. B* 1984; 30: 5596-5610.

298

299

[12] Arčon I, Kodre A, Abra RM, Huang A, Vallne JJ, Lasič DD, *Colloids and Surfaces B: Biointerfaces*, 2004, 33, 199-204.

300

301

[13] Meng W, Xiao D, Wang R. Enhanced production of tetramethylpyrazine in *Bacillus licheniformis* BL1 by *bdhA* disruption and 2,3-butanediol supplementation. *World J. Microbiol. Biotechnol.* 2016; 32: 32-46.

302

303

304

[14] Kozjek Škofic I, Padežnik Gomilšek J, Kodre A, Bukovec N, *Solar Energy Materials & Solar Cells*, 2010, 94, 554-559.

305

306

[15] Bouvier P, Djurado E, Ritter C, Dianoux AJ, Lucazeau G. Low temperature phase transformation of nanocrystalline tetragonal ZrO<sub>2</sub> by neutron and Raman scattering studies. *Int. J. Inorg. Mater.* 2001; 3: 647-654.

307

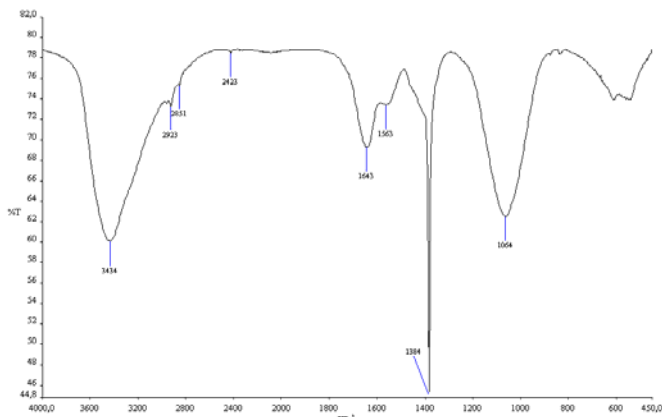
308

309

[16] Coey JMD. The crystal structure of Rh<sub>2</sub>O<sub>3</sub>. *Acta Cryst.* 1970; B 26: 1876-1877.

310

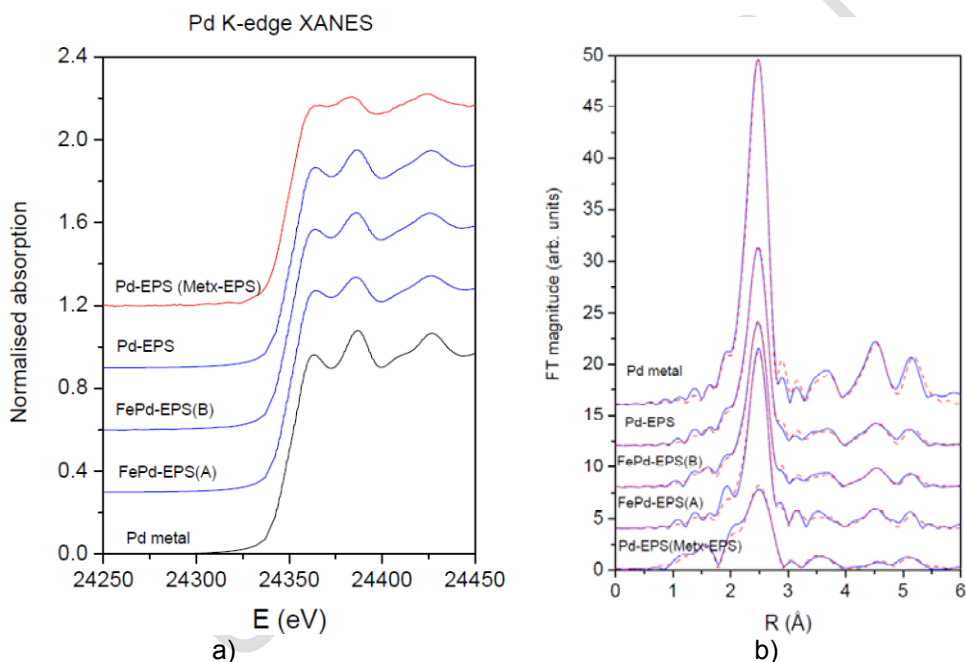
311 APPENDIX  
312  
313



314  
315  
316 **Fig. 1.** FT-IR spectrum of Met<sub>x</sub>-EPS  
317

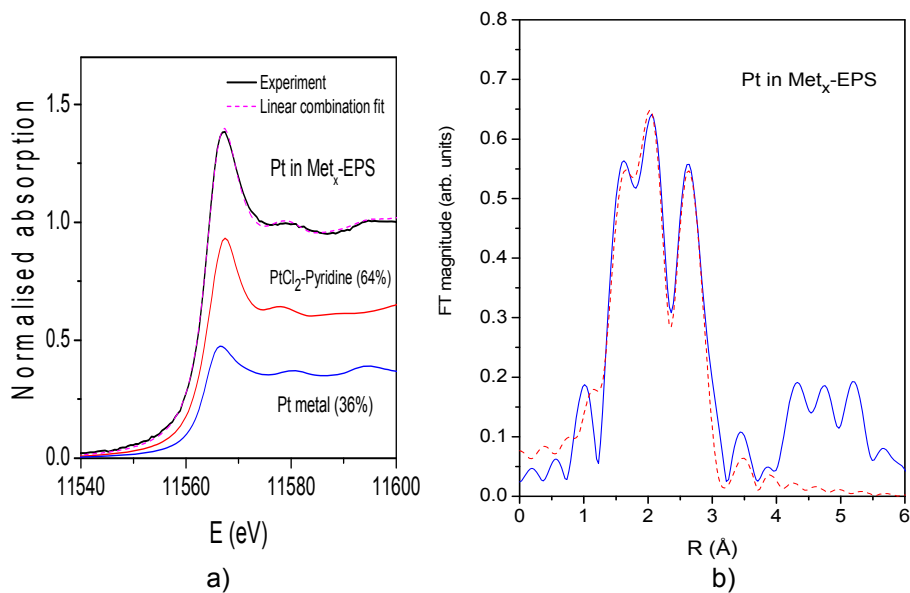
REVIEW

318

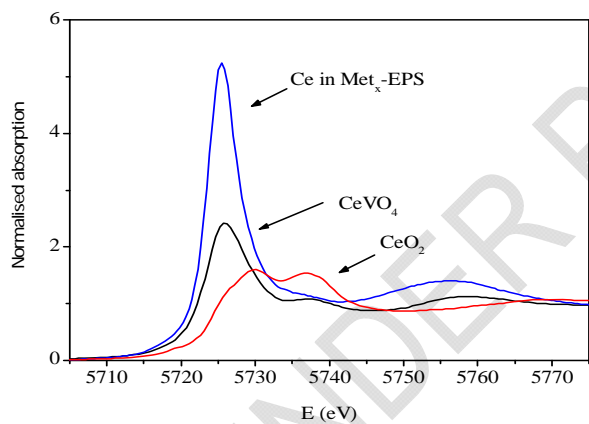


319  
320  
321  
322  
323  
324  
325  
326  
327  
328

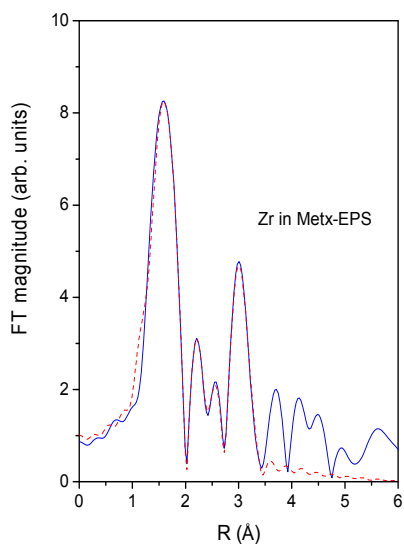
**Fig. 2.** a) Pd K-edge XANES spectra of the Pd-species in Met<sub>x</sub>-EPS sample compared to Pd-EPS, FePd-EPS(A), FePd-EPS(B) samples and reference Pd metal foil with f.c.c. crystal structure; b) Pd EXAFS Fourier transform magnitude of k<sup>3</sup>-weighted Pd EXAFS spectra of Pd-EPS, FePd-EPS(A), FePd-EPS(B), Pd-species in Met<sub>x</sub>-EPS samples and Pd metal foil, calculated in the k range 3–16 Å<sup>-1</sup> and R range 1–5.5 Å. Experiment: solid line; best-fit EXAFS model of the nearest coordination shells: dashed line.



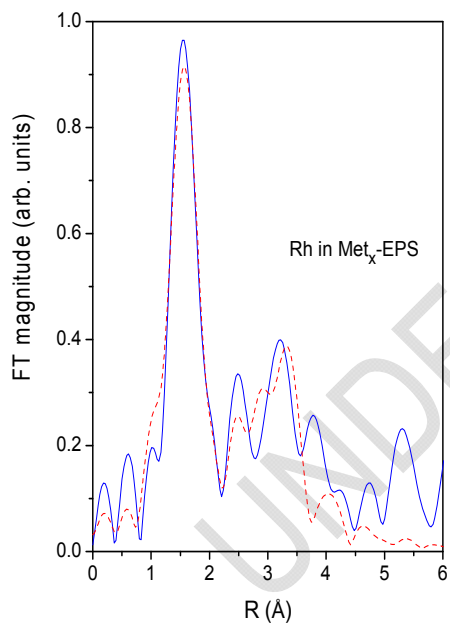
329  
 330  
 331  
 332 **Fig. 3. a)** Pt L3-edge XANES spectrum measured on the Pt in Met<sub>x</sub>-EPS sample: Black solid line: experiment; magenta  
 333 dashed line: best-fit linear combination of XANES profiles of Pt fcc metal (36%), and cis-dichlorobis pyridine platinum  
 334 reference compound (64%); **b)** Fourier transform magnitude of k<sup>2</sup>-weighted Pt L3-edge EXAFS spectra of Pt in Met<sub>x</sub>-EPS  
 335 sample, calculated in the k range 3–12 Å<sup>-1</sup> and R range 1–3.8 Å. Experiment: solid line; best-fit EXAFS model of the  
 336 nearest coordination shells: dashed line.



341  
 342  
 343 **Fig. 4.** Ce L3-edge XANES spectra of the Ce species in Met<sub>x</sub>-EPS sample compared to CeVO<sub>4</sub> and CeO<sub>2</sub> spectra as  
 344 references for Ce<sup>3+</sup> and Ce<sup>4+</sup>, respectively.



348  
 349 **Fig. 5.** Fourier transform magnitude of  $k_3$ -weighted Zr K-edge EXAFS spectra of Zr in  $\text{Met}_x$ -EPS sample, calculated in the  
 350  $k$  range  $3\text{--}11 \text{ \AA}^{-1}$  and  $R$  range  $1\text{--}3.4 \text{ \AA}$ . Experiment: solid line; best-fit EXAFS model of the nearest coordination shells:  
 351 dashed line.  
 352  
 353  
 354  
 355  
 356  
 357



358  
 359 **Fig. 6.** Fourier transform magnitude of  $k_2$ -weighted Rh K-edge EXAFS spectra of Rh in  $\text{Met}_x$ -EPS sample, calculated in  
 360 the  $k$  range  $3\text{--}11 \text{ \AA}^{-1}$  and  $R$  range  $1\text{--}3.4 \text{ \AA}$ . Experiment: solid line; best-fit EXAFS model of the nearest coordination shells:  
 361 dashed line.  
 362  
 363  
 364  
 365

366 **Table 1.** Parameters of the nearest coordination shells around Pd atoms in Met<sub>x</sub>-EPS sample and in reference Pd metal  
 367 foil with fcc crystal structure (a=3.8900 Å): average number of neighbour atoms (*N*), distance (*R*), and Debye-Waller factor  
 368 ( $\sigma^2$ ). Uncertainty of the last digit is given in parentheses. A best fit is obtained with the amplitude reduction factor  $S_0^2 =$   
 369 0.87. The goodness-of-fit parameter, *R*-factor, is given in the last column.

Pd neigh.	<i>N</i>	<i>R</i> [Å]	$\sigma^2$ [Å <sup>2</sup> ]	<i>R</i> -factor
Pd in the Met <sub>x</sub> -EPS sample				
O	1.4(2)	1.97(1)	0.005(2)	
Pd	0.6(3)	3.50(4)	0.008(4)	
Pd	5.3(6)	2.749(4)	0.0075(6)	0.014
Pd	4(2)	3.91(1)	0.013(1)	
Pd	7(2)	4.77(1)	0.013(1)	
Pd	7(3)	5.53(1)	0.013(1)	
Reference Pd metal foil				
Pd	12	2.745(2)	0.0058(2)	0.003
Pd	6	3.896(2)	0.0086(5)	
Pd	24	4.772(2)	0.0088(5)	
Pd	12	5.510(2)	0.0090(5)	

371

372

373 **Table 2.** Parameters of the nearest coordination shells around Pt atoms in Met<sub>x</sub>-EPS sample: average number of  
 374 neighbour atoms (*N*), distance (*R*), and Debye-Waller factor ( $\sigma^2$ ). Uncertainty of the last digit is given in parentheses. A  
 375 best fit is obtained with the amplitude reduction factor  $S_0^2 = 0.91$ . The goodness-of-fit parameter, *R*-factor, is given in the  
 376 last column.

Pt neigh.	<i>N</i>	<i>R</i> [Å]	$\sigma^2$ [Å <sup>2</sup> ]	<i>R</i> -factor
N	1.2(3)	2.04(3)	0.002(1)	0.02
Cl	1.2(3)	2.37(4)	0.003(4)	
Pt	7(3)	2.71(1)	0.013(1)	
C	4.6(8)	2.97(7)	0.003(2)	

378

379

380

381

382

383